

# Coupled Simulation of the System “Workpiece – Dies – Forging Press” by Finite Element Model

Alexey Vlasov <sup>1)</sup>, Alexandr Maximov <sup>2)</sup>, Gunter Lehmann <sup>3)</sup>, Stanislav Dedov <sup>3)</sup>

<sup>1)</sup> Moscow State Industrial University, Moscow / Russia; vav23@mail.msiu.ru

<sup>2)</sup> QuantorForm, Moscow / Russia; info@qform3d.com

<sup>3)</sup> TU Bergakademie Freiberg, Freiberg/Germany

## Summary

The paper presents development and implementation of the methods for simulation of metal forming processes where the material flow problem is coupled with thermal and mechanical solutions in the tool set and in a forging press. This method opens the way to analyse the influence of forming load value and the location of its application on die deformation and press components deflection that is important for precise forging technology. The model is realized in environment of new version 7.0 of QForm2D/3D software.

## 1. Introduction

The simulation of hot metal forming processes in most cases can be done using the assumption that the deformed material is a rigid-plastic continuum while the dies are rigid bodies. Nevertheless there are many cases where such simplification may result in inadequate accuracy. For example, the die deformation in cold forging may be significant comparing to the product tolerances and must be taken into account during simulation of such processes. In case of hot forging the location of the die cavity with respect to press central axis may vary significantly. This causes non-axial loading of the press that in turn results in its uneven deformation. To provide control of press deformation that is vital for precision forging technology the whole system “workpiece – dies – forging press” is to be simulated using coupling of both mechanical and thermal problems.

To be able to deal with these tasks it is necessary to provide the material flow simulation coupled with the tools deformation as it is described in present work. New version of QForm software gives the ability to solve such kind of problems. Example below presents simulation results of mechanical and thermal interaction between workpiece deformation process and behavior of 10MN hydraulic press installed in laboratory of Institut für Metallformung in TU Bergakademie Freiberg.

## 2. Constitutive equations and models

### 2.1. Rigid viscoplastic formulation for deformable work piece.

Deformable material is considered as incompressible rigid-plastic continuum where elastic deformations could be neglected. Constitutive equations for this material according to Levi – von Mises law

$$\sigma'_{ij} = \frac{2\bar{\sigma}}{3\dot{\bar{\varepsilon}}} \dot{\varepsilon}_{ij} \quad (1)$$

where  $\sigma'_{ij}$  and  $\dot{\varepsilon}_{ij}$  – components of stress and plastic strain-rate tensors,  $\sigma'_{ij}$  – deviatoric stress tensor,  $\bar{\sigma}, \dot{\bar{\varepsilon}}$  – effective stress and strain-rate in deforming body. Expression for flow stress  $\sigma$  is presented as

$$\sigma = \bar{\sigma}(\bar{\varepsilon}, \dot{\bar{\varepsilon}}, T) \quad (2)$$

where  $\bar{\varepsilon}$  – effective strain,  $T$  – temperature.

### 2.2. Elastic formulation for equipment and tool

In case when elastic strain components are to be taken into account the model described by the system of equations (1)–(5) is to be modified and complemented by elastic governing equations according to Hook's law

$$\begin{aligned} \sigma'_{ij} &= 2G\varepsilon'_{ij} . \\ \sigma_o &= K\varepsilon_V \end{aligned} \quad (3)$$

where  $G$  is the shearing elastic module,  $\varepsilon'_{ij}$  is the deviatoric elastic strain tensor,  $\sigma_o$  is the mean stress,  $K$  is volumetric elastic module,  $\varepsilon_V$  is the volumetric elastic strain.

### 2.3. Coupled deformation

One of the problems for solution problem of coupled elastic and plastic deformations appears due to different terms of behavior description: plastic behavior is formulated in terms of stress-strain rate (1) and elastic behavior is formulated in terms of stress-strain (3). Another problem is calculation time in the case of joining up of all plastic and elastic deformed objects. To overcome this problem another approach was suggested.

The deformed shape of the tools is the result of application of the load from the deformed body to the tool surface. This deformed shape can be used for the simulation of the material flow at the next time increment. Schematic diagram of this procedure is shown on *Figure 1*. Let  $u_i$  be the present displacements at time  $t_i^e$ . Difference between elastic solution  $u_i^*$  for current load  $P_i$  and this value is

$$\Delta u_i = u_i^*(P_i) - u_i \quad (4)$$

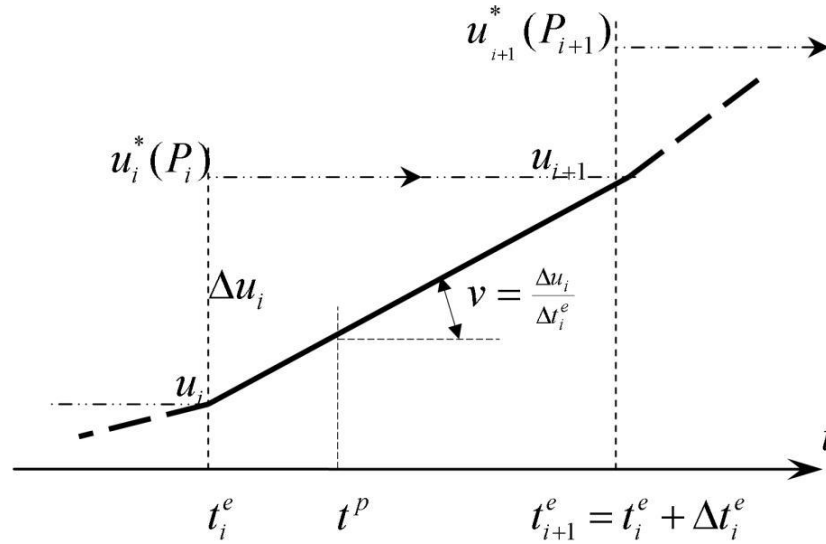


Figure 1. Schematic diagram for solution of coupled elastic-plastic deformation problem

Bild 1. Schematische Darstellung der Aufgabenlösung für gekoppelte elastisch-plastische Deformation

Elastic solution  $u_i^*$  is to be found using expressions (3). Additional velocities of tool points during time increment  $\Delta t_i^e$  could be defined as

$$v_{\text{add}} = \frac{\Delta u_i}{\Delta t_i^e} \quad (5)$$

Value of  $\Delta t_i^e$  is independent with time increment for solution of plastic problem. The velocity  $v_{\text{sum}}$  of any point on the tool surface is the sum of its velocity as a rigid body  $v_{\text{die}}$  plus the velocity of its elastic deformation  $v_{\text{add}}$  in the same point:

$$v_{\text{sum}} = v_{\text{add}} + v_{\text{die}} \quad (6)$$

Thus synchronous displacement of work piece and tool surfaces is guaranteed. Appropriate time step gives the value of additional velocity  $v_{\text{add}}$  that does not exceed the tool velocity as rigid body.

With such approach it is not necessary to combine all deformed bodies into a single system that may significantly increase the simulation time especially for plastic iteration procedure. Even though with this approach we get additional inaccuracy caused by the use of the load from previous configuration the error is supposed to be insignificant due to use of small time increments.

## 2.4. Coupled thermal problem

Energy balance equation for thermal problem in work piece is

$$\rho c \dot{T} = (kT_i)_{,i} + \beta \bar{\sigma} \dot{\epsilon} \quad (7)$$

where  $\beta$  – heat generation efficiency ( $\beta = 0.9 - 0.95$ ),  $\rho$  – density,  $c$  – specific heat and  $k$  – thermal conductivity.

Similar equation, but without the last term is valid for the thermal problem in the tools, where is no heat generation due to plastic work inside of the body.

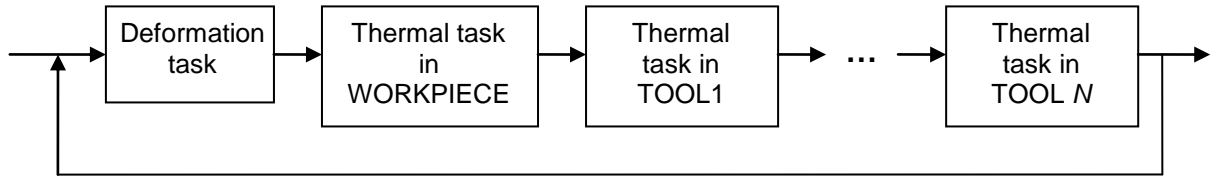


Figure 2. Sequential solution for coupled thermal problem in workpiece and tools

Bild 2. Logische Arbeitsschritte zur Aufgabenlösung für gekoppelte elastisch-plastische Deformation

Coupled simulation is performed by sequential solving of the thermal problem (Figure 2) in the workpiece and then in the tools using actual boundary conditions on their surfaces that include heat flux due to convection, radiation and heating up due to friction.

## 2.5. Assembled dies, multiple deformed bodies

When simulating the tools set consisting of several parts assembled together an additional condition is to be applied on the adjacent surfaces of the contacting bodies. It is the non-penetration condition of the bodies inside each other that can be expressed as the following:

$$u_n^1 = u_n^2 \quad (8)$$

where  $u_n^i$  is normal component of displacement of the body number  $i$ .

Numerical realization of this condition requires special finite elements (Figure 3), consisting of the contacted node  $\mathbf{P}^1$  and the triangle basis with this node projection point  $\mathbf{P}^2$ . The normal load  $P_n$  that takes place on the contact is calculated using penalty method

$$P_n = c(u_n^1 - u_n^2) \quad (9)$$

where  $c$  is positive number that is much bigger than diagonal terms of the stiffness matrix.

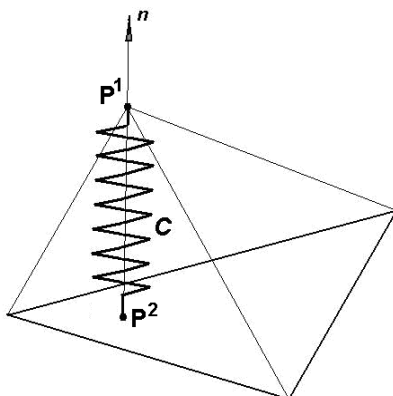


Figure 3. Special contact penalty element for 3D problems

Bild 3. Darstellung eines speziellen Kontaktelementes für 3D-Berechnung

The contact conditions in tangent direction are realized through Coulomb friction law for the contacting parts of the assembled tools

$$P_t = \mu P_n \quad (10)$$

where  $P_t$  is nodal friction force,  $\mu$  is friction coefficient.

### 3. Example of modeling with QForm3D v.7

Example of application shown below presents simulation results of mechanical and thermal interaction of the system workpiece – equipment during forging on hydraulic press 10 MN (*Figure 4*).

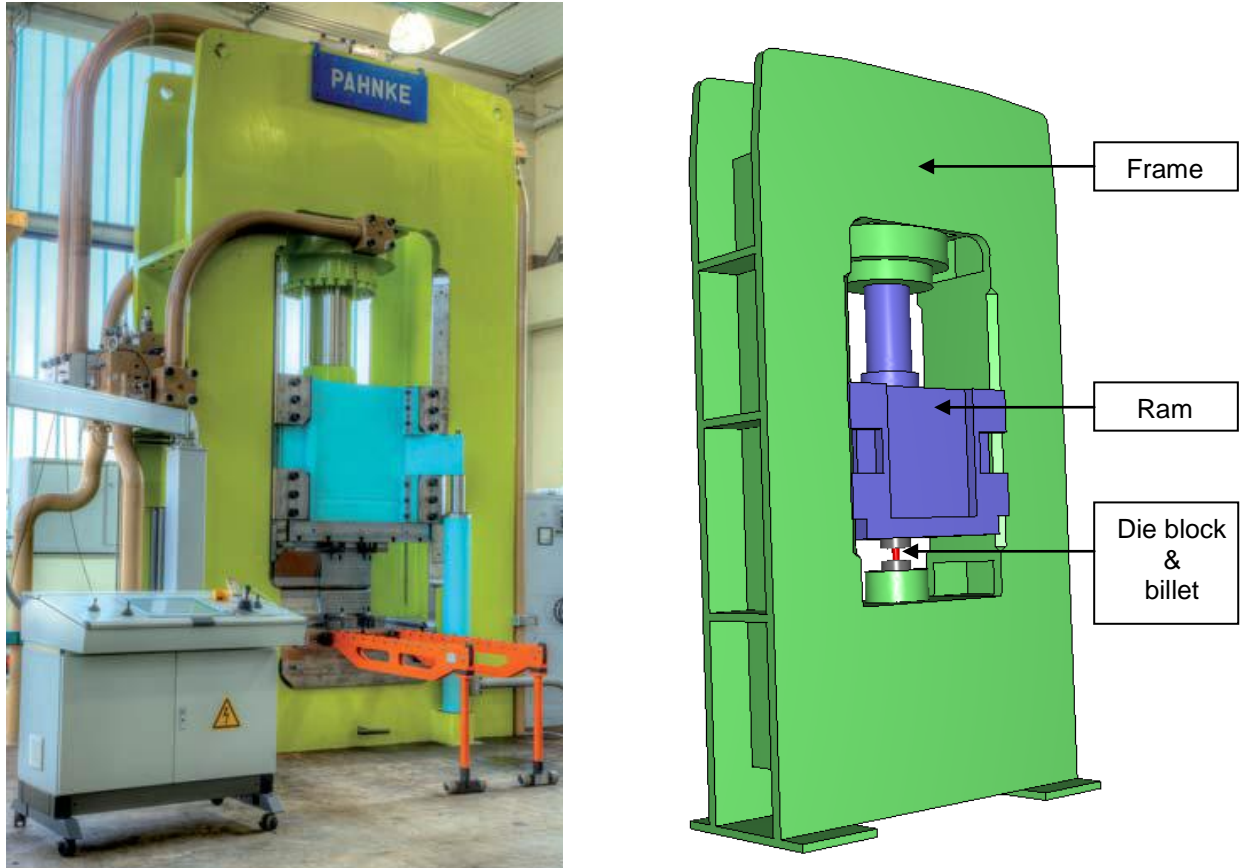


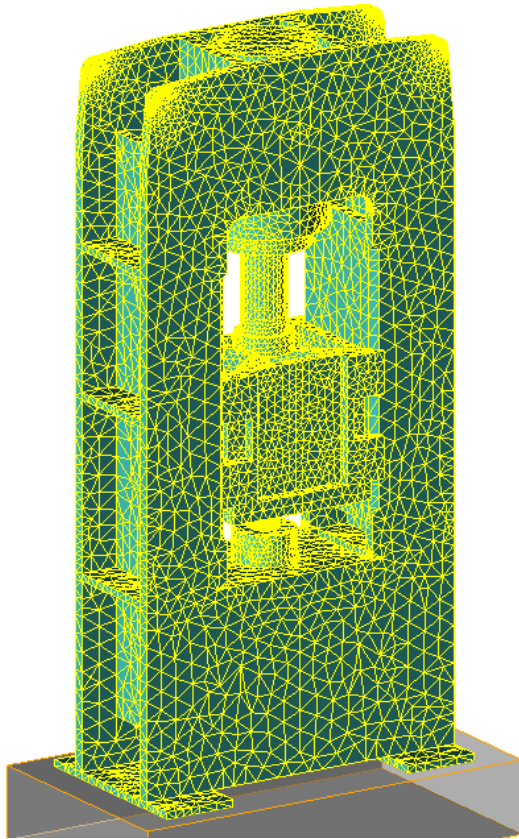
*Figure 4. General view of hydraulic press 10 MN at Institute for Metalforming TU Freiberg (left) and its simplified geometry model for simulation (right)*

*Bild 4. Hydraulische Presse 10 MN Institut für Metallformung TU Freiberg (links) und Vereinfachtes Modell der Presse für Berechnung (rechts)*

To make the simulation easier real design of the press has been simplified omitting some parts that does not provide load bearing functions. Simulation model of press consists from five parts:

- merged frame included press frame, hydraulic cylinder, bottom platen and die holder;
- merged ram included piston, piston shaft, press ram, slides and upper platen;
- upper die;
- bottom die;
- billet.

Number of nodes and linear tetrahedral elements in the mesh required for simulation (*Figure 5*) are given in table.



Simulation part	Number of nodes	Number of elements
merged ram	6449	23152
merged frame	14888	52021
upper die	25169	118057
bottom die	37810	185346
workpiece	3045... 26934	12158... 11677

Figure 5. Finite element mesh for coupled deformation problem

Bild 5. FEM-Benetzung der Presse

Data for simulation:

Yield stress of billet material made of 16CrMn4 was defined as following function

$$\sigma = 1150 \bar{\varepsilon}^{0.07} \exp(-0.07 \bar{\varepsilon}) \dot{\bar{\varepsilon}}^{0.15} \exp(-0.0027 T) \quad (11)$$

Initial temperature for the billet was 1150°C, for the die block was 250°C, for the frame and the ram was 20°C. The feet of press frame were fixed. Press was loaded by the deformation force and pressure in hydraulic cylinder. Properties of the material used for all equipment components include Young's modulus  $2.16 \cdot 10^5$  MPa and Poisson's coefficient 0.33.

The following three examples were solved for a coupled problem "workpiece – dies – forging press" with the QForm3D v.7. They clearly demonstrate an interaction among these three elements.

### 3.1. Example 1: Central mounting of the die

The simulation of the forging process of the part, shown in *Figure 6*, has been carried out. Two technological schemes have been used, i.e. finish forging in one blow and two blows forging with preliminary upsetting.

The forging block and billet were placed on the symmetry axis of the press, as shown in *Figure 5*. The tool velocity was 250 mm/s. In both cases the workpiece was placed 5 mm out of the die axis, in order to cause an asymmetrical load condition.

In one blow forging process the workpiece moved to the die center in the very beginning of the process due to the geometry of the upper tool *Figure 4*.

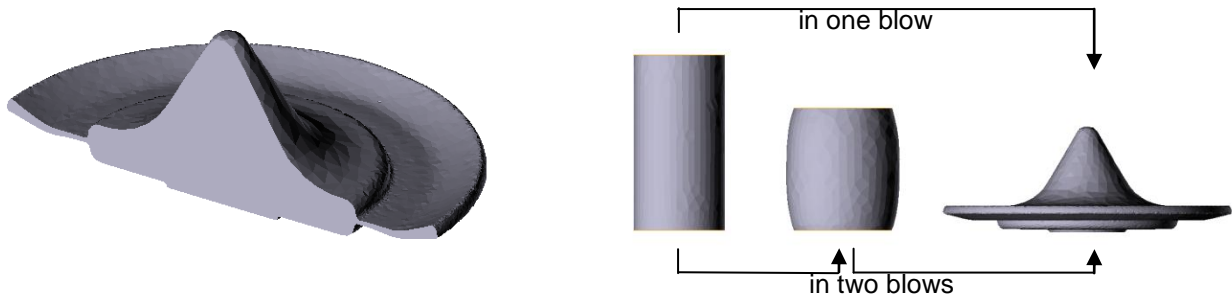


Figure 6. The forged part and two technological processes of its production

Bild 6. Fertiges Schmiedeteil (links) und Formänderung nach zwei Umformschemen (rechts)

The same occurred during the second step in two blow process, the pre-deformed workpiece moves to the center of the die. So further process in both cases occurred practically under a symmetrical load condition.

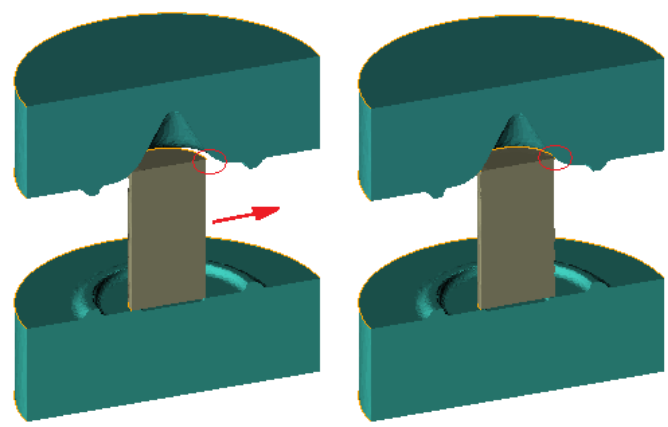


Figure 7. Self-centering of work piece at the beginning of forging process

Bild 7. Selbstzentrierung des Umformrohlings am Anfang des Schmiedevorgangs

The load curves for the both process schemes are shown on the Figure 8. The zero load stage at the beginning of the curves (approximately 0.01 s) corresponds to the self-centering movement of the workpiece.

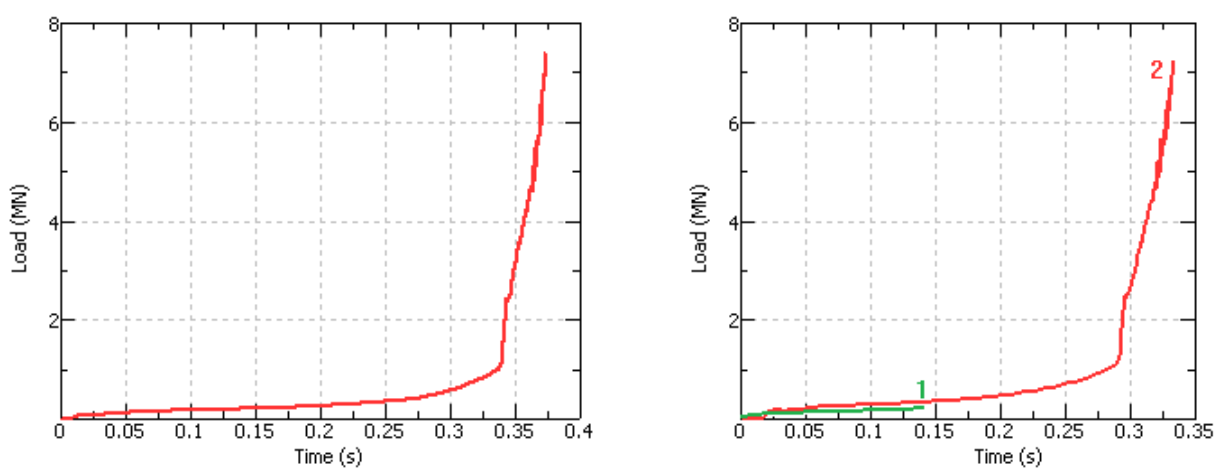


Figure 8. Load curve of one blow (left) and two blow (right) forging process (1 – upsetting and 2 – finish forging)

Bild 8. Kraftverlauf beim Pressvorgang in einem Umformschritt (links) und in zwei Umformschritten (rechts, 1 – Vorstauchen und 2 – Fertigschmieden)

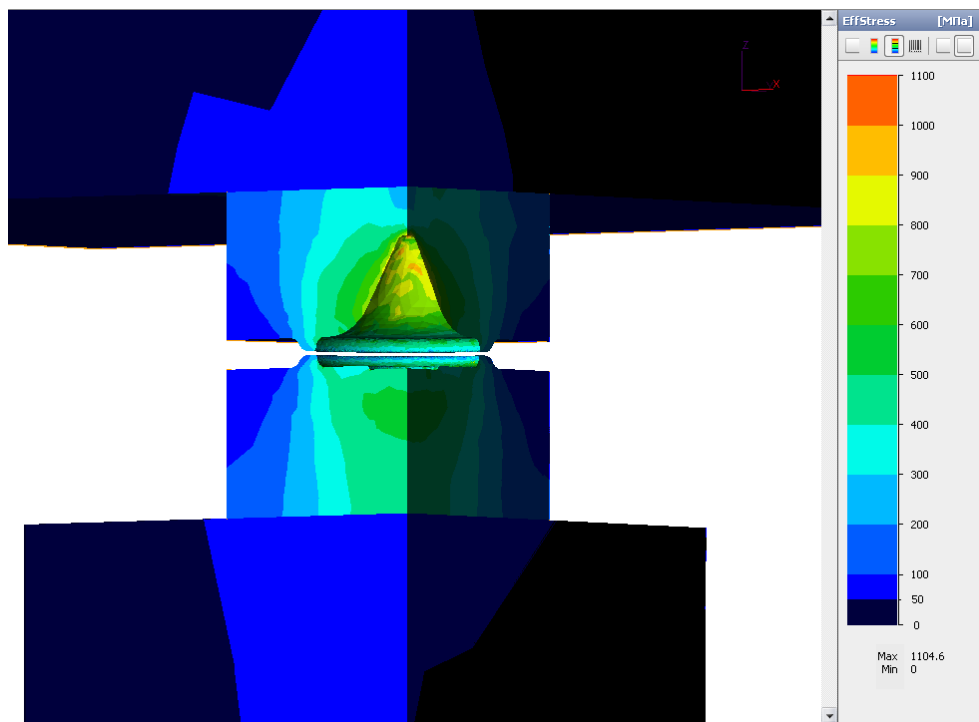


Figure 9. Effective stress distribution in the tool during the forge process

Bild 9. Spannungsfeld im Umformwerkzeug beim Schmiedevorgang

The maximal load of 7.19 MN was reached at the end of the one blow forging. In the case of the two blows forging process the load of the first blow was 0.24 MN (green curve), and the 7.25 MN of the second one. So the loads at the end of the processes are nearly the same. For that reason the further simulation results are very similar.

Figures 9 and 10 show the effective stress and vertical displacements of the equipment.

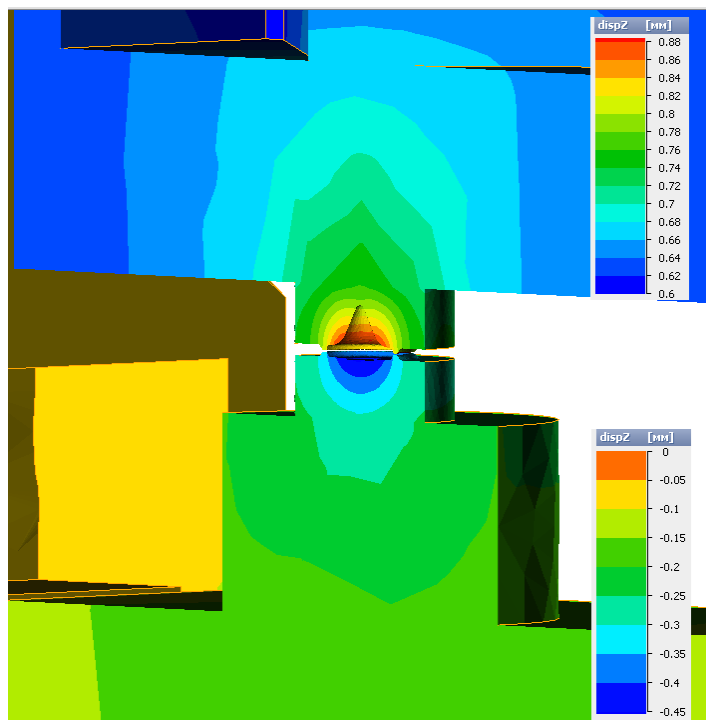


Figure 10. Tool displacement during the forge process

Bild 10. Verschiebung der Werkzeuge beim Schmiedevorgang

As depicted in the picture the maximal effective stress achieves 1105 MPa at the top part of the upper die. This value is less than yield stress of the die material. Under symmetrical load conditions the maximal local displacements reaches 0.83 mm in the upper tool (lateral surface) and -0.42 mm in the lower tool (central point). On the gutter zone they are 0.76 mm and -0.30 mm correspondingly. It means that total high of the workpiece will be approximately 1.1 mm greater than nominal size. Local dimensions can differ on additional 0.2 mm. It is necessary to note that the most part of this displacements come from deformation of the ram and frame (0.69 mm and -0.25 mm correspondingly)

### 3.2. Example 2: Off centre position of the tools

The further examples demonstrate the results in case of off-centre positions of the forging tools. The technological process was the same as in example 1. Due to the asymmetrical loading conditions there are noticeable displacements in the different parts of the frame of the hydraulic press. The highest displacement values along X- and Z-axes reach 0,017 and 0,055 mm respectively (*Figure 11*). The press frame bends opposite to loaded side.

### 3.3. Example 2: Off centre position of the tools

The further examples demonstrate the results in case of off-centre positions of the forging tools. The technological process was the same as in example 1. Due to the asymmetrical loading conditions there are noticeable displacements in the different parts of the frame of the hydraulic press. The highest displacement values along X- and Z-axes reach 0,017 and 0,055 mm respectively (*Figure 11*). The press frame bends opposite to loaded side.

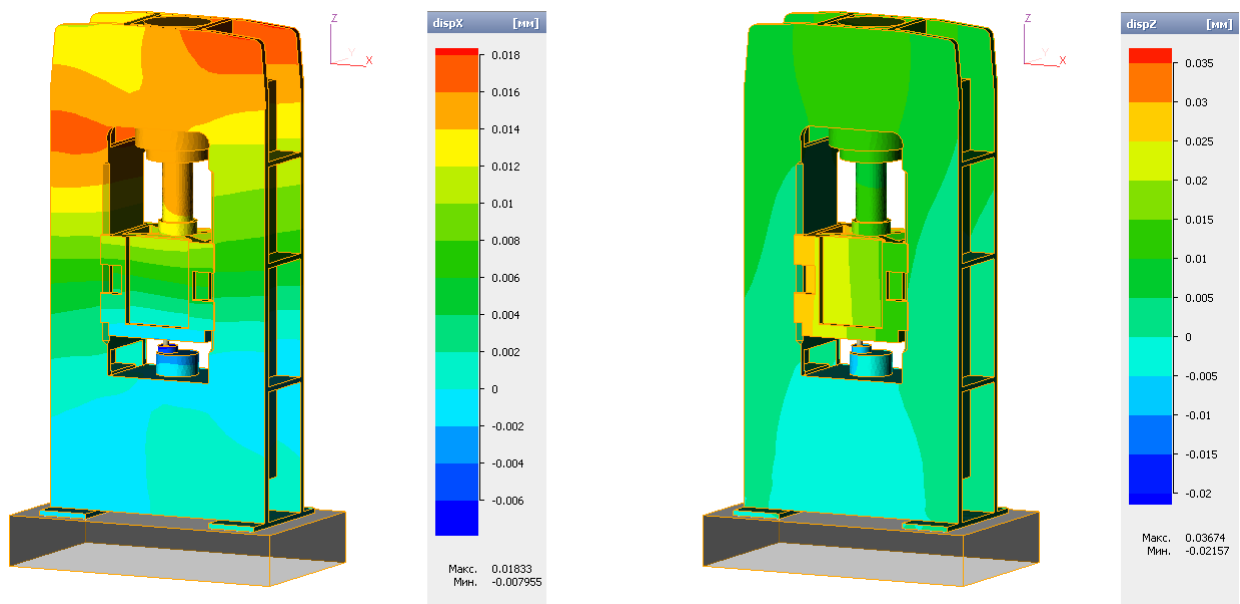


Figure 11. Horizontal (left) and vertical (right) displacement of the press frame caused by the off-centre positioning of forging tools

Bild 11. Wage- und senkrechte Verschiebung des Pressrahmens durch seitliches Anbringen des Werkzeugs

### 3.4. Example 3: Thermal loading of the tools

The following example demonstrates results of a thermal loading of the tools due to contact with a hot workpiece.

Two thermal tasks were calculated:

- a) thermal loading during just one blow forging cycle (0,37 s)
- b) thermal loading by being in contact with the forges workpiece for 100 s that represents several forging cycles in a raw..

In the first case due to low contact time the temperature of the cavity surface rose from 250 to 370°C for upper die and to 600°C for lower die while there is no material heating at some depth (*Figure 12*).

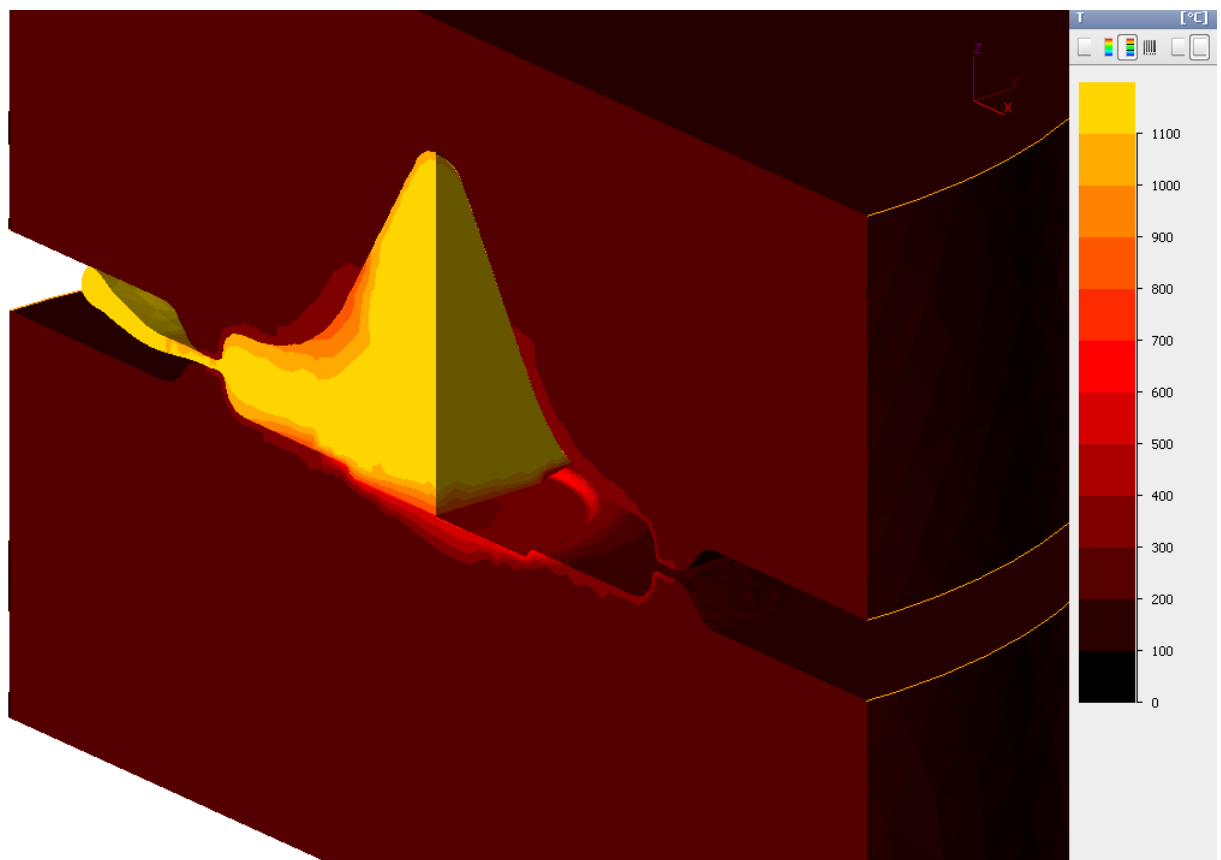


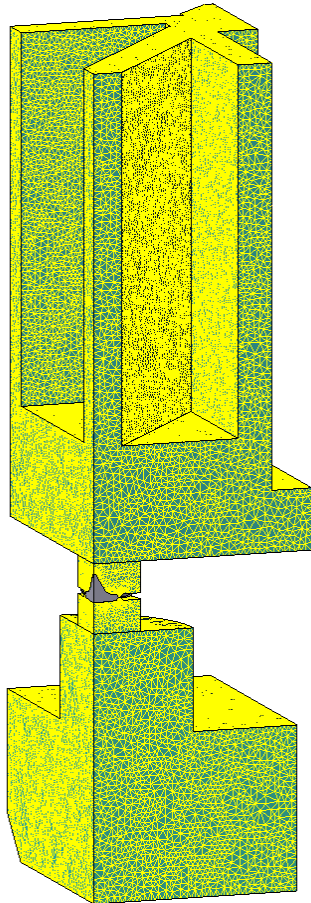
*Figure 12. Temperature field in the die set (half cross-section) and workpiece (quarter) after single forging process*

*Bild 12. Temperaturfeld im Werkzeug und Werkstück nach einem Schmiedevorgang*

For solving of the long thermal loading case (case “b”) special fine size FEM-mesh has been used (*Figure 13*).

The results are shown on *Figure 14*. According to simulation results of QForm the temperature of the tools firstly rises and then reaches an equilibrium state between the heating by the workpiece and cooling by the environment. This procedure takes about 70 s. After that the cavity surface achieves approximately 950°C and the temperature at the tool mounting surface is about 350°C.

The heat flux into the ram is much lower and its highest temperature does not exceed 150°C.



Simulation part	Number of nodes	Number of elements
ram	68876	340639
platen	26074	130665
upper die	4414	20029
bottom die	5609	26154

Figure 13. Finite element mesh for coupled thermal problem and its parameters

Bild 13. FEM-Benetzung für die Lösung der thermischen Aufgabe

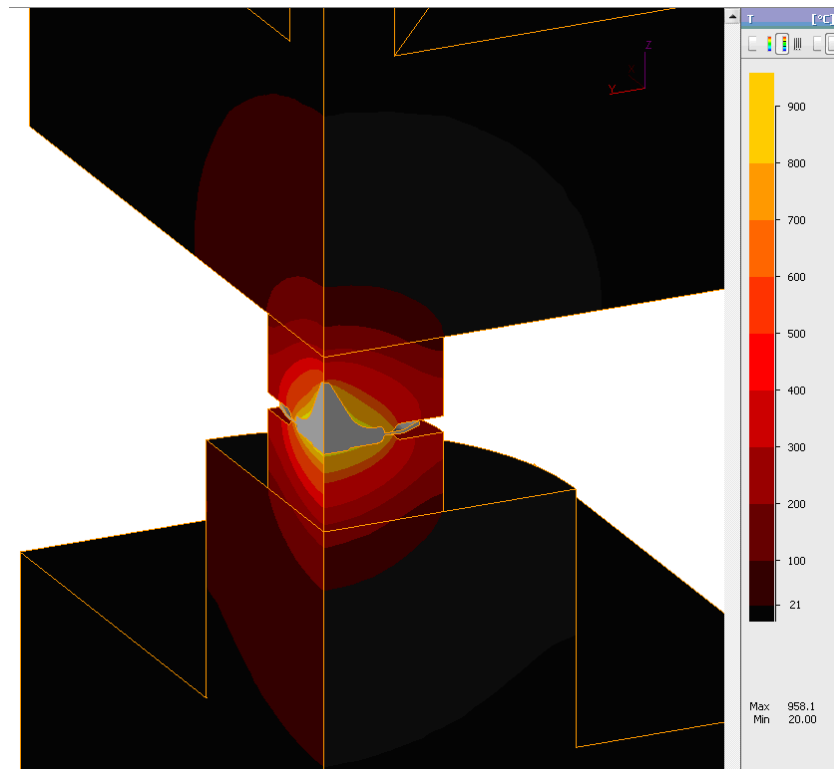


Figure 14. Temperature distribution when thermal equilibrium has been reached by long contact time between the tools and workpiece

*Bild 14. Temperaturverteilung im Werkzeug beim durch lange Kontaktzeiten erreichten  
Temperaturgleichgewicht zwischen Werkzeug und Werkstück*

## **4. Conclusion**

Mechanically and thermally coupled model has been developed and tested in a new version 7 of QForm3D software. A forging process coupled with deformation of hydraulic 10 MN press of Institute of Metalforming TU Freiberg has been modeled.

The tests have shown that elastic deformation of the dies and the press itself may have great influence on the simulation accuracy when forging the parts with high requirements to finish geometry like, for example, turbine blades. Thermal coupling allows more accurate calculating of the distribution of the temperature in the dies and workpiece and provides the background for prediction of the thermal cracks and fatigue in case if respective material models can be incorporated. These results also provide background for implementation of model of microstructural evolution in the workpiece that is available in QForm3D [3].

## **References**

1. Biba N., Stebunov S., Lishny A., Vlasov A. New approach to 3D finite-element simulation of material flow and its application to bulk metal forming, 7<sup>th</sup> International Conference on Technology of Plasticity, 27 October – 1 November, 2002, Yokohama, p. 829–834.
2. Biba N., Stebunov S., Vlasov A. Material forming simulation environment based on QForm 3D software system. 12<sup>th</sup> International Conference Metal Forming 2008, 21–24 September, 2008. Vol. 2, p. 611–616.
3. Borowikow A., Wehage D., Biba N. Simulation of Thermo-Mechanical Treatment in Industrial Manufacturing Processes. 10<sup>th</sup> International Conference on Technology of Plasticity. Aachen, Germany. 25–30 September, 2011. p. 826–831.